

1 Targetless image-based method for measuring displacements 2 and strains on concrete surfaces with a consumer camera

3
4
5
6
7 Belen Ferrer¹, Pablo Acevedo², Julian Espinosa², David Mas²

8
9 ¹Dept. Civil Engineering, Universidad de Alicante. PO BOX 99, 03080 Alicante (SPAIN)

10
11 ²Ins. Physics Applied to Sciences and Technologies, Universidad de Alicante. PO BOX 99,
12 03080 Alicante (SPAIN)

13 14 15 16 17 18 19 20 21 22 23 24 25 26 27 28 29 30 31 32 33 34 35 36 37 38 39 40 41 42 43 44 45 46 47 48 49 50 51 52 53 54 55 56 57 58 59 60 61 62 63 64 65

ABSTRACT

10 Measurement of concrete strain through non-invasive methods is of great importance in civil
11 engineering and structural analysis. Traditional methods use laser speckle and high quality
12 cameras that may result too expensive for many applications. Here we present a method for
13 measuring concrete deformations with a standard reflex camera and image processing for
14 tracking objects in the concretes surface. Two different approaches are presented here. In the
15 first one, on-purpose objects are drawn on the surface, while on the second one we track small
16 defects on the surface due to air bubbles in the hardening process. The method has been tested
17 on a concrete sample under several loading/unloading cycles. A stop-motion sequence of the
18 process has been captured and analyzed. Results have been successfully compared with the
19 values given by a strain gauge. Accuracy of our methods in tracking objects is below 8 μm , in
20 the order of more expensive commercial devices.

21
22
23 **Keywords:** Concrete, Strain measurement, Non contact measurement , Image Processing, Stop
24 motion, Targetless method, Centroid calculation

1. INTRODUCTION

Measurement of concrete strain is a most important subject in civil structures. It can be used as an indirect measure of the concrete stresses, thus giving important information about the condition of the structure. Additionally, it can be also used to detect movements or vibrations on the structure.

Traditionally, the measurement of concrete strain is done using contact sensors like strain gauges. A strain gauge is a flexible long sheet with a foil pattern printed on the surface. This sheet is glued to the concrete surface using a cyanoacrylate adhesive. When concrete stress changes, the thickness of the foil changes and it changes its resistance. A Wheatstone bridge can measure this change in resistance, which is related to the strain. Due to its own nature, small changes in temperature affect the measurement, as well as humidity. Therefore, despite their high accuracy, strain gauges are very sensitive to climatic conditions.

Non-invasive procedures are generally preferred because there is no expensive disposable material when the experiment is destructive (concrete samples). Additionally, non-contact procedures do not need physical access to the target point so their use does not interfere with the normal use of the structure. Moreover, they are independent on the external conditions like temperature or humidity. These characteristics make non-contact procedures safer and more convenient than the rest of procedures.

Non-contact procedures are mainly based on vision systems. These systems are being fast developed in the latest years due to the increasing cameras performances and calculation capacity of the computers. In the literature some new developments based on image techniques can be found. One of the image techniques that have been used to measure concrete strain is based on the sampling moiré method [1]. It uses a regular repeated pattern based on lines with different grey levels as a target on the structure. The relative movement of the lines gives information about the deformations on the sample. Based on this technique, Umemoto et al. [2]

1 have developed a new method to measure strains just using a sticker on the surface to be
2 measured. The big advantage of this method is that the simple visualization of the sticker allows
3 obtaining the measurement, but still it needs a target to be glued on the surface.

4 Video extensometers are also being used for measuring the strain on different materials (usually
5 metals). These systems use fiducial marks on the material that are tracked with a high-quality
6 camera and software analysis. Usually, Digital Image Correlation (DIC) has been used as a
7 useful tool in the measurement of both displacement and strain [3-5]. In many works, instead of
8 fiducials, speckle pattern generated by a laser beam is used to improve the accuracy of DIC
9 measurements [6]. A simpler alternative, known as pseudo-speckle consists of making a similar
10 pattern by painting a cloud of random spots on the concrete surface under study. In any case, on
11 purpose patterns must be placed or projected on the concrete surface.

12 Targetless methods have been recently presented in the literature. These methods do not need an
13 object or a special pattern attached to the specimen, but search for illumination changes [7] or
14 defined shapes [8] such as screw heads or holes that are identified and used as targets.

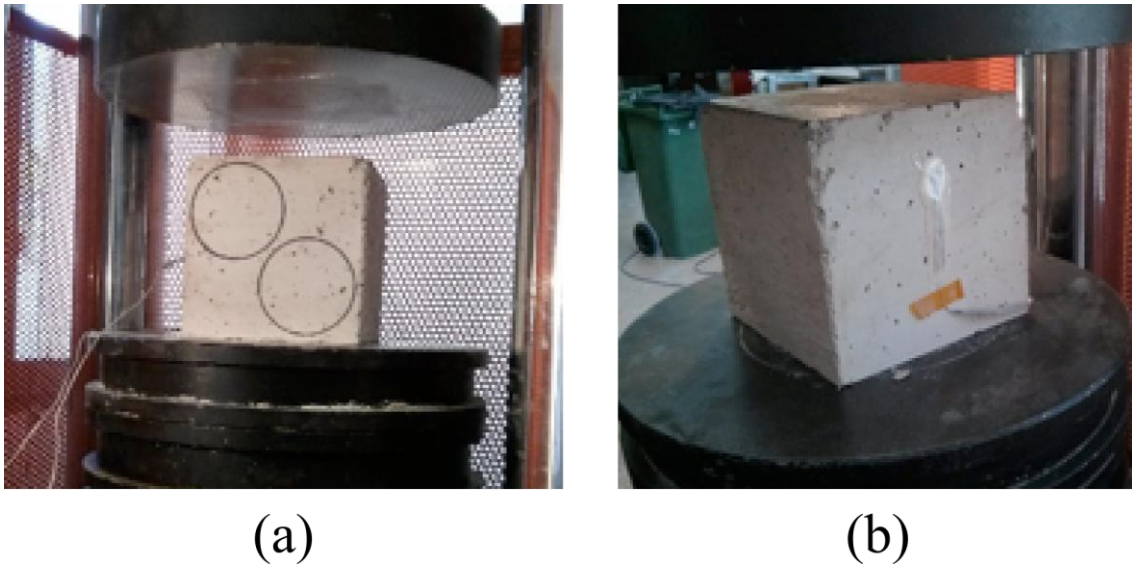
15 In this work we develop a new procedure to measure concrete strain without the use of any
16 particular target, shape or projected pattern on the concrete surface. Our approach consists of
17 extracting information from the surface texture i.e. the own roughness of the concrete surface.
18 Concrete surface usually shows some superficial irregularities, due to a non-perfect compaction
19 during the placement of concrete into the formwork. The most common superficial irregularities
20 are small holes with irregular shapes and distribution, corresponding to air bubbles that have
21 been trapped during the process. These holes could affect the concrete durability, since they
22 allow air and contaminants to enter into the material but their effect is negligible from the point
23 of view of concrete strength. To avoid these irregularities a very accurate compaction is needed,
24 covering both needle vibrator (with a proper quantity per concrete volume to compact) and
25 vibrating tables to apply vibration to the formwork. This technique, widely used in precast
26 concrete elements, is difficult to apply in big elements that are built on site. Therefore, these

1 superficial irregularities happen very often and they are commonly consented. Anyway, the
2 method presented here could use any superficial irregularities like humidity spots, furrows or
3 even changes of color.

4 The aim of this paper is to show that these irregularities can be tracked and, from their position,
5 the concrete strain can be obtained. Additionally we show that the method can be implemented
6 on video sequences obtained from a standard reflex camera working in stop-motion mode.
7 Through image processing algorithms defects of larger size are recognized and segmented from
8 each frame. Then, they are identified as individual blobs and its position is determined. By
9 analyzing the relative distances between them we are able to determine the concrete strain. All
10 image processing is done with Matlab [9] by using the Image and Signal Processing toolboxes,
11 together with our own developed software. Our results are successfully compared with those
12 coming from a strain gauge, thus proving that our method is accurate and reliable.

14 2. METHOD

15 A video sequence of a concrete cubic sample subjected to several load-unload cycles is
16 obtained. Two methods will be used here: one consists of using circles drawn on the concrete
17 surface as targets, while the other one uses the small defects on the concrete surface. Picture
18 sequences from a lateral face of the sample have been analyzed and processed as explained
19 below. Additionally, a strain gauge was glued to the sample in order to obtain reference results
20 (see figures 1a and b)



1
2
3
4
5
6
7
8
9
10
11
12
13
14
15
16
17
18
19
20
21
22
23
24
25
26
27
28
29
30
31
32
33
34
35
36
37
38
39
40
41
42
43
44
45
46
47
48
49
50
51
52
53
54
55
56
57
58
59
60
61
62
63
64
65

Figure 1 Concrete sample used in the test (a) Frontal view with two targets drawn on it, (b) Rear view with the strain gauge.

1
2
3
4
5
6
7
8
9
10
11
12
13
14
15
16
17
18
19
20
21
22
23
24
25
26
27
28
29
30
31
32
33
34
35
36
37
38
39
40
41
42
43
44
45
46
47
48
49
50
51
52
53
54
55
56
57
58
59
60
61
62
63
64
65

Let us consider any of the pictures in figure 1. One can see there the circles made with a marker and the small superficial defects that appear as dark objects against a more or less uniform background. This kind of images provides a clear bimodal histogram, as can be seen in figure 2a with the main lobes describing the scene background (highest peak) and foreground respectively. Thresholding is automatically done according to Otsu's method, which calculates the optimum threshold level separating the two object classes so that their intra-class variance is minimum [10]. The binary frame so obtained may permits classification and isolation of target objects from the concrete surface as can be seen in figure 2b.

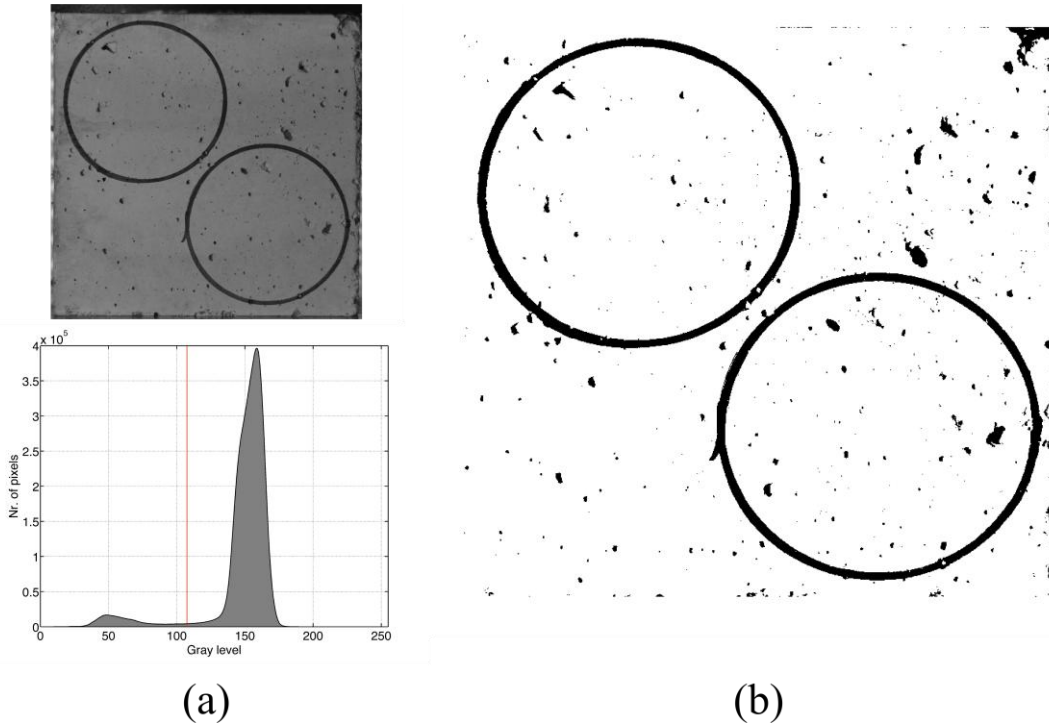


Figure 2 (a) Gray scale picture of the probe and histogram. The vertical line marks the Otsu's optimum threshold at level 107. (b) Binarized version of the frame.

Regions are identified, labeled and tracked by algorithmic applications of graph theory [11]. A graph is a representation of a set of objects where some pairs of objects are connected by links. Here primary objects are white pixels and the links between them are established according to connectivity between objects. In this sense, two pixels can be 4-connected or 8-connected depending whether they are orthogonally adjacent or also in diagonal (see figure 3). Therefore, all pixels surrounding one target-pixel are 8-connected with it, but not all of them are 4-connected. Therefore, once the complete image is analyzed and the graph is constructed, several groups of connected pixels are detected over the background. On this work each one of these group is called "blob".

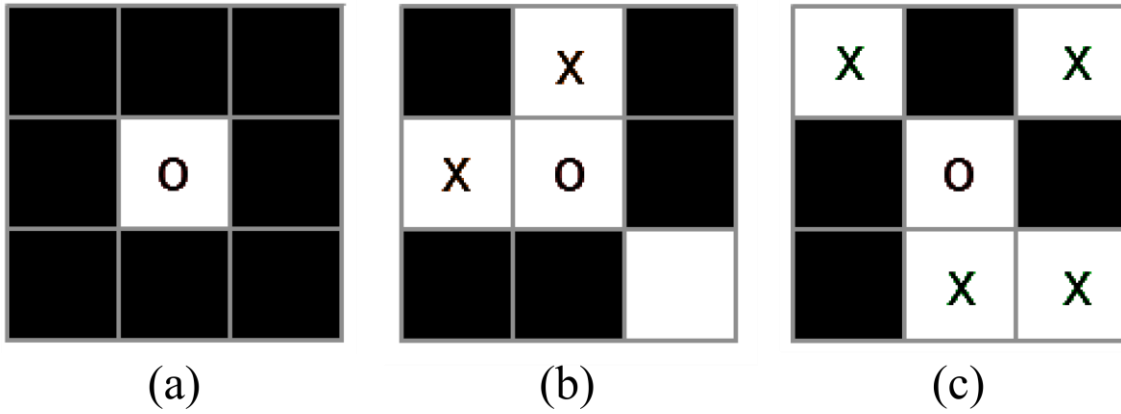


Figure 3 (a) Isolated pixel. (b) 4-connected pixels marked with X; (c) 8-connected pixels marked with X. Notice that according to these definitions, a pixel in diagonal is not 4-connected with the central one but 8-connected.

In our case, regions or blobs are defined by grouping 8-connected pixels. These regions are individually labeled and their geometrical features are calculated (area, centroid, major and minor axes, eccentricity...). From these features, only the centroid will be relevant for our calculations here.

The procedure just described can provide very noisy results. From all the blobs detected, very small regions can alter its form or even disappear during the process. Therefore, only regions within an area range are selected and tracked along the process.

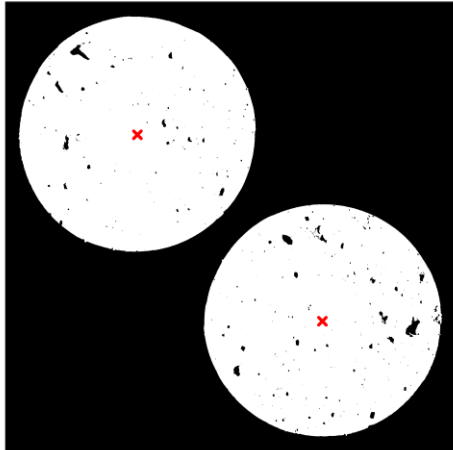
When concrete is subjected to strain, the distance between any centroids in the direction of the strain changes. Once the location of two centroids throughout the time (t) is known, the length (l) of a line in the direction of the strain can be determined simply by subtracting the locations.

The strain is then calculated by dividing the increment of length at a particular time by the initial length, as it is described in equation 1.

$$e(t) = \frac{l(t) - l(t_0)}{l(t_0)} \quad (1)$$

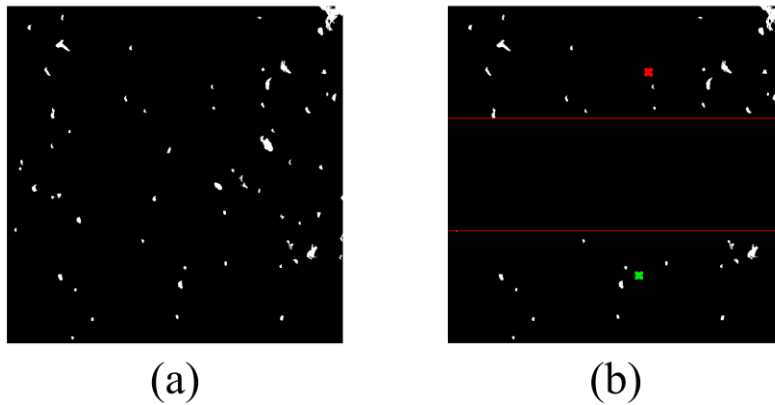
1 As we said before, two different approaches have been adopted here. The first approximation
2 imposes two specific regions artificially designed so detection is easier and the procedure is
3 easier checked and followed.

4 In the first approach, using two circles as objects, the regions are formed by the encircled pixels
5 and the drawn line breaks connectivity with other regions (see figure 2b). Notice that aside of
6 the two encircled region, the remaining white pixels also form a region. By filtering all regions
7 whose area is below 20 % or above 25% of the total concrete area we select the two regions of
8 interest, as it is represented in figure 4. The regions selected have been on purpose-built in an
9 elliptical shape. Small stains inside these regions can be easily erased by using a closing
10 morphological filter [12]. Then, the contour of each region can be extracted and fitted to an
11 ellipse by following the procedure described in [13]. The centroid is then calculated from the
12 obtained ellipse parameters and distance between them in the vertical coordinate is used to
13 obtain the strain as stated in expression (1).



14
15 **Figure 4** Blobs (white area) obtained from the binarized image in figure 2 using a size range
16 from 20% to 25% of the complete concrete area. The X symbol marks the calculated centroid.

1 In the second approach, we identify and track the superficial defects in the concrete. Since we
2 have defined the regions as formed by white pixels over a black background, we have inverted
3 all the frames in the sequences, in order to have the object to be tracked in white pixels. Again,
4 blobs can be selected by its size, which in this case ranges from 0.03% to 0.5% of the image
5 size (figure 5a) in order to detect the defects in the concrete surface as blobs. Contrary to the
6 previous case, these blobs have not a defined shape. Since these regions are of small size, any
7 pixel variation due to the illumination or small camera movement may affect to the centroid
8 location thus producing a noisy signal. Notice that contrary to the drawn-circumference case,
9 now we will usually have more than two blobs distributed over the whole surface. Hence, the
10 problem of selecting two blobs to define a length to compute the strain with equation (1) arises.



11 (a) (b)
12 **Figure 5** (a) Blobs (white areas) obtained using a size range from 0.03% to 0.5% of the
13 complete concrete area. (b) Regions, delimited by the red line, and blobs used to calculate the
14 region centroid which is pointed with an X

15
16 To obtain a single displacement measurement and reduce the location error, we have considered
17 not single blobs but two groups of them and the center of each group is calculated. Notice that
18 the farther the groups are, the higher will be their relative displacement, and consequently, the
19 lower is the error. Therefore the simplest approach is dividing the whole area in three equal
20 horizontal regions as it is shown in figure 5b and taking the upper and lower parts. Since each
21 area contains several blobs, their mean position is calculated and compared with its counterpart.

1 Changes in concrete strain are thus determined by the relative position of the mean value of the
2 centroids coordinate of the upper and lower parts. From this point, as in the previous procedure,
3 using equation (1) the strain is straightaway calculated.

4 The measurements are compared with a 50 mm length strain gauge that was glued in the
5 opposite side of the cubic sample (figure 1b). The value given by this strain gauge was recorded
6 at a rate of one per second and it was compared with those from the camera.

7 Finally, we must add that the method is fully automatic. The captured sequence, composed by
8 around 700 pictures, each one with a resolution of 16 Mpx was processed off-line. The
9 software only requires a previous calibration to establish the pixel to mm ratio and then the size
10 of the object areas in order to select the proper regions. Thresholding and calculations are done
11 automatically. The process took 1225 sec (1.7 sec per frame) on a laptop running Windows 7
12 with a Core I5 processor, 4 GB RAM and SSD hard disk.

14 3. EXPERIMENTAL SET UP AND RESULTS

15 We prepared a series of cubic concrete samples, with lateral length of 15 cm, which were
16 subjected to loading-unloading compression cycles. The concrete was poured in the formwork
17 in two layers, consolidating each one by hitting the lateral walls of the formwork with a rubber
18 mallet. First of all, in order to know the strength characteristics of concrete, compression failure
19 test were done on 3 of these samples, showing an average failure strength of 28.44 MPa, thus
20 giving a total load of 640 kN needed to make fail the 15 cm side cubic sample.

21 Four experiments were done using the same concrete sample, to be sure that the results are
22 repeatable. In these experiments, the concrete sample was subjected to five cycles of
23 compression loading and unloading. The speed in both loading and unloading tasks was 5 kN/s

1 and the maximum load reached in every cycle was of 400 kN, which is smaller than the yield
2 limit for the concrete used in these experiments. With the strain gauge we determined that the
3 maximum strain reached in the load-unload cycles was 800 $\mu\epsilon$. In the last experiment the
4 loading was maintained, at the same rate, until the concrete failure, which happened at 680 kN.

5 During the loading cycles, we took one image per second using time lapse with a Nikon 5100
6 camera which has an 18-55 mm lens and a spatial resolution of 16 Mpx. Although most cameras
7 are able to record videos sequences, the standard formats limit the resolution to 1080 vertical
8 lines, thus making frame resolution of around 2Mpx. Still images offer much higher resolutions
9 but at lower frame rate. Thus, the camera was configured in a stop-motion mode taking 1 picture
10 per second. The camera distance together with the zoom used gives a minimum field of 160 mm
11 in the vertical direction, being the conversion ratio of 19.65 px/mm.

12 The accuracy of the method was determined by analyzing a static sequence, i.e. the concrete
13 sample is captured with no force applied on it. Therefore, variations on the position of the
14 centroids are due to inaccuracies of the method, and not to any displacement in concrete. Thus
15 error of the method will be taken as the standard deviation of the measurement taken in static
16 conditions.

17 In the first approach we drew two circles of 80 mm of diameter in the frontal surface of the
18 concrete samples. The accuracy in the determination of the ellipse center is 0.08 px, which
19 means that the method has a spatial accuracy of 4 μm . Regarding the strain, the measurement
20 composition according to expression (1) increases the error, thus giving an error of 20 $\mu\epsilon$.

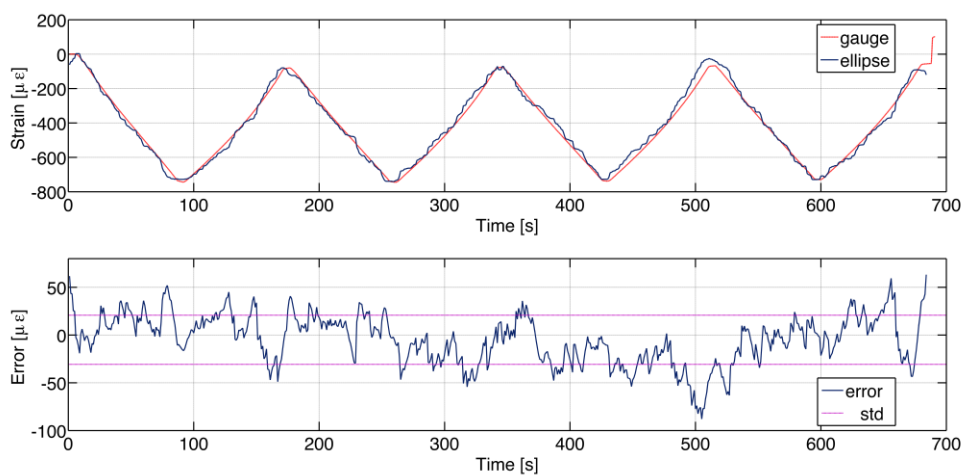
21 In the second approach, the regions are much smaller so errors due to misclassified pixels are
22 proportionally larger. In this case, the accuracy in determining the centroid of the upper and
23 lower regions from the blobs is around 0.15 px, which means an accuracy of around 8 μm . The
24 accuracy of the method for determining the strain is around 40 $\mu\epsilon$.

1

2 3.1. Results from ellipse fitting

3 As we said above, strain on the concrete has been calculated from the upper and lower ellipse
 4 centroids. Results from the strain gauge were directly obtained from the measuring unit.
 5 Although different experiments were done, we only represent here one of them, since results
 6 were statistically equivalent. In figure 6 we represent the results given by the strain gauge and
 7 the ellipse centroids. As it can be seen there, results are in very good agreement. Errors between
 8 both methods have also been depicted together with the standard deviation.

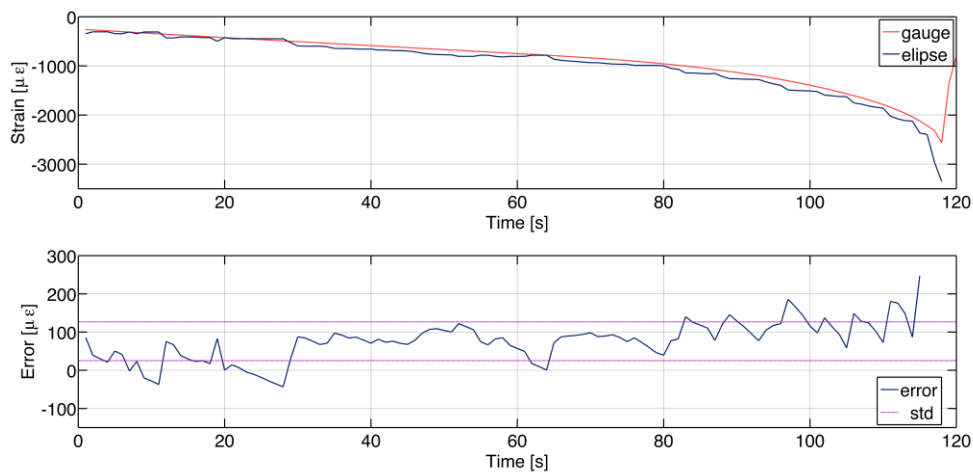
9 In general, errors fluctuate in the $\pm 50 \mu\epsilon$ band, being the largest difference $87 \mu\epsilon$ in absolute
 10 value, corresponding to the peak around 500 s. In average, the error of our method compared
 11 with the strain gauge is of $-5 \pm 25 \mu\epsilon$ (mean \pm standard deviation). Relative errors are difficult to
 12 estimate due to presence of small strains, which may distort the results. Anyway, excluding the
 13 first 10 data due to division by zero, the relative error is between 6% and 10%. Finally, notice
 14 that the accuracy obtained is in agreement with the values previously determined with the static
 15 sequence.



16

1 **Figure 6** Comparison between strain gauge and two circles centroids method for five cycles of
 2 loading and unloading. The standard deviation is marked with two lines in the error graph.
 3 Mean value has not been represented since it is indistinguishable from the axis line.

5 In the last experiment, the sample was compressed until its failure. The results obtained by
 6 using the ellipse fit are shown in figure 7. There we also depict the difference between our
 7 method and the reference. The absolute difference fluctuates in the $\pm 100 \mu\epsilon$ interval while the
 8 absolute value of the strain is lower than $2000 \mu\epsilon$. From that point, the error increases very fast
 9 until the failure point, where the deviation is really large. Excluding the last four data points
 10 from the measurement with the camera, the error for this experiment is $-1 \pm 50 \mu\epsilon$.

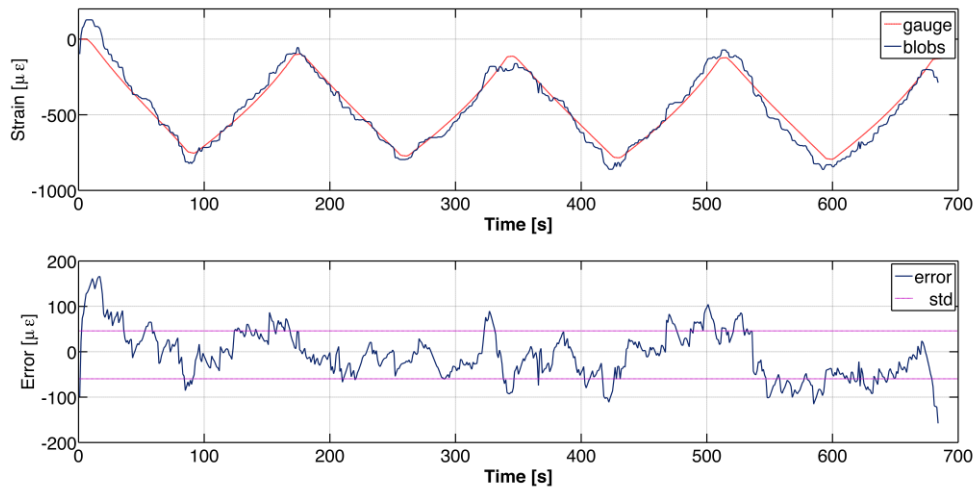


12 **Figure 7** Comparison between strain gauge and two circles centroids method for loading until
 13 concrete failure. The last 4 points from the image method, around the failure region, have been
 14 excluded from the error analysis. The standard deviation is marked with two lines in the error
 15 graph. Mean value has not been represented since it is indistinguishable from the axis line.

17 3.2. Results from blobs tracking

18 From the acquired video-sequences, the strain has been recalculated but now using the regions
 19 obtained from the defects on the concrete surface, as it was explained above. As in the previous

1 case we have represented the results obtained with our method together with those coming from
 2 the gauge (see figure 8). Despite the fact of being noisier than the previous method, the signal
 3 still follows the load/unload cycle. In this case, the absolute error has its maximum in $160 \mu\epsilon$,
 4 which is 2 times higher than the maximum absolute error obtained by using two circles centroid.
 5 The mean and standard deviation of the error method was $-7 \pm 50 \mu\epsilon$ while the relative error
 6 obtained in four experiments was around 14%.



7

8 **Figure 8** Comparison between strain gauge and the tracking-blobs method for five load-unload
 9 cycles. The standard deviation is marked with two lines in the error graph. Mean value has not
 10 been represented since it is indistinguishable from the axis line.

11

12 Using this method with the images taken during the loading until failure, the obtained strain is
 13 shown in figure 9. The maximum absolute error is around $150 \mu\epsilon$, while the measured strain is
 14 lower than $2000 \mu\epsilon$. From that point, the absolute error increases very fast. Excluding the failure
 15 region, as we did in the previous case, the error of this method in this experiment is $4 \pm 50 \mu\epsilon$.

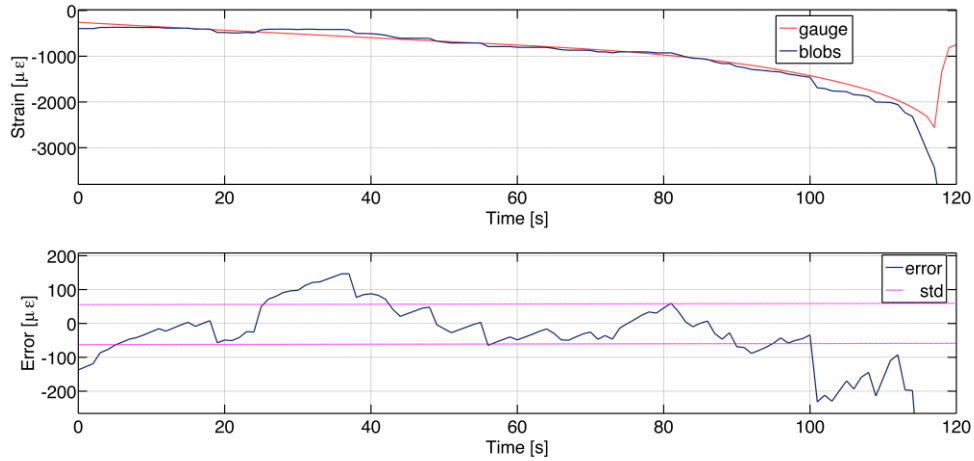


Figure 9 Comparison between strain gauge and superficial entities method for loading until concrete failure. The last 4 points from the image method, around the failure region, have been excluded from the error analysis. The standard deviation is marked with two lines in the error graph. Mean value has not been represented since it is indistinguishable from the axis line.

4. DISCUSSION

The experiments just exposed show that our proposal is accurate enough to measure the concrete strain. As we expected, method based in the ellipse fitting is more accurate than the blobs tracking. On the one hand, circles are of known shape and this information is used to determine its center by minimum squares fitting while calculation of the centroid of a blob group is just an averaging operation. Therefore, the larger size of the regions and the additional constrains on the object shape help to decrease the errors.

On the other hand, drawing the ellipses needs direct access to the concrete surface. Although this is easily done in the lab, measurement of real structures may not be so simple so application of this technique is not always possible. On those cases, targetless methods are preferred even if their accuracy is lower. Additionally, image processing and computational complexity of the second method is less demanding so results are faster to obtain.

1 With the two techniques analyzed, we showed that the method is capable of reproducing the
2 load-unload cycles. Mean values of the error are always lower than $10 \mu\epsilon$ (in absolute value)
3 while standard deviations are between $25 \mu\epsilon$ and $50 \mu\epsilon$ depending on the method and the
4 experiment. Errors in general are random so we could not detect any systematic bias of the
5 optical method compared with the traditional strain gauge.

6 Notice that when the concrete strain goes over the yield limit, the difference between the video
7 techniques and the strain gauges increases. This behavior was detected in both proposed
8 techniques and may be due to the disaggregation of some parts of the sample, which affects the
9 concrete surface that is being analyzed.

10 In any case, we would like to underline that, although the absolute error is higher around the
11 failure point, so is the strain and, as a consequence of this, the relative error still remains around
12 10%. Despite of this, we can underline one of the advantages of our method since the sequence
13 can be reviewed and the exact failure moment can be easily visualized.

14 Regarding the performance of our system compared with other devices, a simple search on
15 commercially available devices show that Video Extensometers using high-resolution cameras
16 provide resolutions of around $2 \mu\text{m}$ (see [14] or visit [15] for a list of suppliers), with a 200 mm
17 field of view. In our case, we have used a standard photo camera that, with a similar field of
18 view, provides accuracies of 4 and $8 \mu\text{m}$, depending in the tracking method selected.

19 The accuracy of our method can be further improved by using raw images. Standard consumer
20 cameras like the one used here usually save pictures in JPEG format, in order to save storage
21 memory. This format usually applies a lossy compression that degrades the image. Compression
22 is done in non-overlapping blocks of 8×8 pixels. This compression introduces some noise in
23 the image and reduces the subpixel accuracy [13]. Nevertheless, although our accuracy is a bit
24 lower, the system cost is much lower, thus the cost-benefit ratio of our proposal results much
25 better.

1 **5. CONCLUSIONS**

2
3
4 2 We have presented an image-based method for measuring deformations and strains on concrete
5
6 3 surfaces. The method is based on detecting pixel clusters on the concrete surface and track them
7
8 4 while a load is applied on the concrete. According to these clusters, the concrete surface is
9
10 5 divided into regions. By calculating the centroid of these regions, we can calculate the
11
12 6 deformation on the concrete due to the loading forces and, from that, the concrete strain.

13
14
15
16 7 Our proposal has been implemented in two different ways with different accuracies. One
17
18 8 implementation consisted on drawing elliptic lines on the concrete contour. This creates two
19
20 9 artificial regions in the concrete surface that can be easily detected and isolated. Since the shape
21
22 10 of these regions is known, their contour can be mathematically described and its centroid
23
24 11 accurately determined.

25
26
27
28
29 12 The second implementation does not require of previously determined regions, but considers the
30
31 13 defects on the concrete surface. By selecting these defects as blob objects, their centroid can be
32
33 14 determined. Then the blobs in the upper and lower part of the concrete surface are grouped and
34
35 15 the average position of the centroid is calculated. By calculating the relative variation of upper
36
37 16 blob cloud with respect to the lower cloud, the concrete strain can be calculated.

38
39
40
41
42 17 Accuracy of both methods is comparable to existing commercial devices based on image
43
44 18 detection (8 μm), although the cost is much lower. In our case, we only need a reflex camera
45
46 19 (600\$) to acquire the images. Sequences are processed off line with our own software developed
47
48 20 in Matlab.

49
50
51
52 21 Finally, we would like to underline that the tracking method is independent of the camera. In
53
54 22 this case we implemented it on a standard consumer photo-camera, working at 1Hz but it can be
55
56 23 also implemented with higher speeds for fast processes. Also the objective can be changed and
57
58 24 thus use the method analyzing microscopic or telescopic sequences. In any case if other

1 cameras, objectives or object distances are used, a static sequence of few frames may be used to
2 calibrate and determine the accuracy of the new set up.

3 The method here explained is applicable to measurements in large structures and buildings, but
4 some previous considerations have to be done. In first place, illumination over the surface may
5 change over time. This may not affect the method since the histogram of each frame is
6 individually analyzed and so is the binary threshold. Other problem that may appear is that the
7 area can be unevenly illuminated. In this case different background subtraction techniques may
8 be used [16]. Therefore, by implementation of convenient image processing methods, the
9 technique can be adapted to different illumination conditions.

10 In second place, as we pointed before, larger magnifications permit more details in the texture
11 but smaller field of view. For large structures, one possible solution is tracking texture details by
12 using sub-pixel techniques [13]. One can also compose a larger scene by taking images with
13 different synchronized cameras. In any case, application of the method to particular concrete
14 structures should be specifically analyzed and it will be addressed in future works.

15 **ACKNOWLEDGMENTS**

16 The authors acknowledge the support of the Spanish Ministerio de Economía y Competitividad
17 through the project BIA2011-22704, the Generalitat Valenciana through the project
18 PROMETEO/2011/021 and GV/2013/009 and the University of Alicante through the project
19 GRE13-10

21 **REFERENCES**

22 [1] Ri S, Fujigaki M, Morimoto Y. Sampling Moiré Method for Accurate Small Deformation
23 Distribution Measurement, Exp. Mech. 2010; 50; 501-508.

1
2
3
4
5
6
7
8
9
10
11
12
13
14
15
16
17
18
19
20
21
22
23
24
25
26
27
28
29
30
31
32
33
34
35
36
37
38
39
40
41
42
43
44
45
46
47
48
49
50
51
52
53
54
55
56
57
58
59
60
61
62
63
64
65

[2] Umemoto S, Tanoue S, Miyamoto N, Takaki T, Ishii I, Aoyama T, Fujii, K. Concrete surface strain measurement using Moiré fringes, *Constr. Build. Mater.* 2014 (in press).

[3] Malesa M, Kujawinska M. Deformation measurements by Digital Image correlation with automatic merging of data distributed in time, *Appl.Opt.* 2013; 52; 4681-4692

[4] Gencturk B, Hossain K, Kapadia A, Labib E, Mo Y. Use of digital image correlation technique in full-scale testing of pre-stressed concrete structures, *Measurement* 2014; 47; 505-515

[5] Verbruggen S, Aggelis DG, Tysmans T, Wastiels J. Bending of beams externally reinforced with TRC and CFRP monitored by DIC and AE, *Compos. Struct.* 2014; 112; 113-121

[6] Wang Z, Kieu H, Nguyen H, Le M. Digital image correlation in experimental mechanics and image registration on computer vision: similarities, differences and complements, *Opt. Laser Eng*, 2014 (in press)

[7] Ferrer B, Espinosa J, Roig AB, Perez J, Mas D. Vibration frequency measurement using a local multithreshold technique, *Opt. Express*, 2013; 21; 26198-26208

[8] Busca G, Cigada A, Mazzoleni P, Zappa E. Vibration monitoring of multiple bridge points by means of a unique vision-based measuring systems, *Exp. Mech.* 2014; 54; 255-271

[9] Matlab (Mathworks Inc.) at <http://www.mathworks.com> (last seen in 07/16/2014)

[10] Otsu N. A threshold selection method from gray-level histograms” *IEEE T. Man. Cyb.* 1979; SMC-9; 62-66

[11] Trudeau RJ *Introduction to Graph Theory*, New York, Dover Pub; 1993

[12] Serra J. *Image Analysis and Mathematical Morphology*, London, Academic Press, 1982

1
2
3
4
5
6
7
8
9
10
11
12
13
14
15
16
17
18
19
20
21
22
23
24
25
26
27
28
29
30
31
32
33
34
35
36
37
38
39
40
41
42
43
44
45
46
47
48
49
50
51
52
53
54
55
56
57
58
59
60
61
62
63
64
65

1 [13] Mas D, Espinosa J, Roig AB, Ferrer B, Perez J, Illueca C. Measurement of wide frequency
2 range structural microvibrations with a pocket digital camera and sub-pixel techniques, Appl.
3 Opt. 2012; 51; 2664-2671
4 [14] Instron at <http://www.instrom.us> (last seen in 07/16/2014)
5 [15] “How sensors work: the video extensometer” <http://www.SensorLand.com> (last seen in
6 07/16/2014)
7 [16] “Background subtraction” http://en.wikipedia.org/wiki/Background_subtraction, (last seen
8 in 10/2/2014)

Highlights

- Strain in concrete is usually measured with resistive gauges
- A non-contact image-based method is presented
- The method is implemented on a standard digital photographic camera
- Accuracy of the method is around 8 μm for displacements and 40 $\mu\epsilon$ for strain
- Results are comparable to alternative commercial devices